

# MPPT Modeling and Simulation in PV Systems Using the DNN Method

Edi Leksono<sup>1</sup>, Robi Sobirin<sup>2</sup>, Reza Fauzi Iskandar<sup>3</sup>, Putu Handre Kertha Utama<sup>4</sup>, Mochammad Iqbal Bayeqi<sup>5</sup>, Muhammad Fatih Hasan<sup>6</sup>, Irsyad Nashirul Haq<sup>7</sup>, Justin Pradipta<sup>8</sup>

<sup>1,2,3,4,5,6,7,8</sup> Department of Engineering Physics, Faculty of Industrial Technology, Institut Teknologi Bandung, Bandung 40132 INDONESIA, (tel.: 022-2504424; fax: 022-2506281, email: <sup>1</sup>edi@tf.itb.ac.id, <sup>2</sup>robisobirin15@gmail.com, <sup>3</sup>rezafauzi@gmail.com, <sup>4</sup>handre.kerthautama@gmail.com, <sup>5</sup>iqbalbayeqi54@gmail.com, <sup>6</sup>fatihhasan029@gmail.com, <sup>7</sup>irsyad.n@office.itb.ac.id, <sup>8</sup>justinpradipta@office.itb.ac.id)

<sup>3</sup> Department of Physics Engineering, Faculty of Electrical Engineering, Universitas Telkom, Bandung 40257 INDONESIA (tel.: 022-756s4108; fax: 022-7562721, email: rezafauzi@gmail.com)

[Received: 25 May 2023, Revised: 12 September 2023]  
Corresponding Author: Edi Leksono

**ABSTRACT** — The maximum power point tracking (MPPT) feature in solar power plants is an essential function in increasing the efficiency of electricity production. The incremental conductance (InC) algorithm controls MPPT, aiming to maximize the output power of photovoltaic (PV) panels and increase the efficiency of the solar power plant system. Even though the InC algorithm is simple and practical, this algorithm tends to lack support in precise switching speeds, is sensitive to the measurement precision level, and is inadequate to eliminate power oscillations due to tight switching cycles. The deep neural network (DNN) algorithm has the potential to answer the challenges of MPPT dynamics. DNN's learning capabilities enable the controller to better recognize the dynamics of shifts in maximum power values, thereby providing more appropriate contact actuation. The input for the DNN is the duty ratio produced by the InC algorithm. The DNN algorithm was implemented on three DC-to-DC power converter topologies, namely buck, boost, and buck-boost, to determine MPPT performance under standard tests and actual environmental conditions. DNN has demonstrated the ability to reduce oscillation effects, speed up steady-state time, and increase efficiency. In actual environmental conditions, the results showed that the buck converter consistently produced the highest power, followed by the boost and the buck-boost converters. Regarding performance efficiency, the buck converter achieved the highest efficiency at 94.58%, followed by the boost converter at 90.79%. Conversely, the buck-boost converter had the lowest performance efficiency, with an efficiency of 79.34%.

**KEYWORDS** — PLTS, MPPT, DC/DC Converter, DNN.

## I. INTRODUCTION

Clean energy is an urgent need and significantly impacts the sustainability of the environment and human life in general. The commitment to the 2016 Paris Agreement regarding the United Nations (UN) framework agreement on climate change is proof of the urgency of every country to reduce CO<sub>2</sub> gas emissions caused using fossil fuels [1]. Various efforts have been made, one of which is by opening access to renewable energy, including promoting the provision of photovoltaic (PV)-based electrical energy. It is evident that there is an increasingly growing support for using solar energy. The costs of PV panels, power electronic devices, and batteries have a tendency to decrease over time. Nevertheless, efforts to increase efficiency remain crucial in minimizing system losses. This issue becomes more prevalent when dealing with changing energy sources and increasingly complex PV system topologies. Based on these conditions, it is clear that the role of maximum power point tracking (MPPT) technology is essential to increasing PV systems' efficiency.

PV performance is influenced by environmental factors, such as solar irradiance and air temperature. Due to their effects on the supply of current, voltage, and electrical power in the PV system, these two environmental variables will impact the performance of PV modules in producing electrical energy. It relates to the current and voltage characteristic curves or current-voltage (I-V) curves on PV panels, which will produce a different maximum power point (MPP) for each solar irradiance condition. Therefore, the urgency of the solar power plant system requires an MPPT controller device to maximize the output value of the PV panel and increase the efficiency of

the solar power system in every weather condition encountered [2].

The MPPT controller used in PV systems basically consists of a particular controller algorithm and a power converter [3]. The algorithms commonly used are conventional algorithms, such as the perturb-observe (PO) algorithm, fuzzy logic, and incremental conductance (InC). These algorithms are responsible for controlling the switching mechanism in the power converter to form a function called a charge controller or regulator of current, voltage, and electrical power. The power converter completes the control algorithm in order to achieve the target voltage or power by selecting a circuit topology with certain features according to needs. However, in the context of MPPT controllers, conventional algorithms cannot completely resolve nonlinearity and oscillation problems caused by rapid changes in environmental conditions, such as changes in solar irradiance and air temperature [2]. InC tends to be simple and practical to implement, but it is important to note that this method does not support precise switching speeds [4] and is sensitive to the level of measurement precision [5]. Similarly, the efficiency of PO tends to decrease, especially in the event of rapid changes in irradiance and temperature due to weather changes [6], slow tracking speed, and steady-state oscillation problems [7]. The issues of oscillation merits consideration as well. A proper control strategy should be able to minimize the occurrence of power oscillations due to tight switching cycles [8].

Machine learning approaches can potentially answer the challenges of MPPT dynamics, such as artificial neural networks (ANN) or deep neural networks (DNN). These

algorithms imitate the working mechanism of the human brain's neural network, which comprises many neurons and nodes. The ANN algorithm is robust and efficient. It works at an optimal point without causing significant oscillations [9], despite its implementation being more complex. DNN offers better ways for overcoming accuracy problems due to the algorithm's increased accuracy and computational speed [2]. The MPPT algorithm with machine learning will maintain the output power at the highest point by combining current and voltage measurements with a switching duty ratio feed [10]. In 2020, a DNN-based MPPT controller algorithm for wind and combined PV/wind energy systems was successfully modeled and demonstrated [10]. A DNN-based MPPT algorithm using MATLAB to improve the quality of output power produced using a combined PV and fuel cell system was successfully developed [11]. Furthermore, in 2022, a study utilized the DNN algorithm in MPPT applications to reduce inappropriate power losses so as to obtain effective maximum power points with less computational error time [12].

This paper focuses on the development of MPPT using the DNN method with the aim of contributing to efforts to reducing converter oscillations and identifying converters with optimal efficiency. Additionally, the DNN structure is expected to be able to reduce iteration routines and computational speed. Writing systematics consists of four main sections: Introduction, Methodology, Testing and Analysis, and Conclusion. In the Introduction section, literature reviews on MPPT issues in general and the urgency of DNN in MPPT are presented. The Methodology section outlines various stages involved in data preparation, system modeling, and the methods used to assess system performance. The Testing and Analysis section explains the results and analysis of MPPT simulations in standard test conditions (STC) and actual environments, respectively, in buck, boost, and buck-boost modes. The Conclusion section explains the efficiency achievements of MPPT-DNN in these three modes.

**II. METHODOLOGY**

**A. DATA UNDERSTANDING AND DATA PREPARATION**

This stage seeks to understand the data configuration used and the data preparation process by selecting and processing data. Solar power plant modeling consists of a PV array model and MPPT system design. The PV array model used Skytech Solar SIM 210 PV modules. The PV module was modeled as a user-defined array with 2 parallel and 16 series arrays. The datasheet components used were adjusted to the parameter blocks in MATLAB, namely rated power, open circuit voltage, short circuit current, the voltage at MPP, current at MPP, and temperature coefficient.

Meanwhile, the data processed as inputs were collected from the results of weather measurements around the measurement area, which were stored in the MySQL database on the phpMyAdmin page. The data used were air temperature and solar irradiance.

**B. MODELING**

The solar power plant system was modelled using the MPPT with Simulink in MATLAB. The constructed system was composed of a PV array, a DC-to-DC power converter, a control algorithm, and a constant-value resistive load, as shown in Figure 1.

The system input was the processed air temperature and solar irradiance data. Using the air temperature and solar

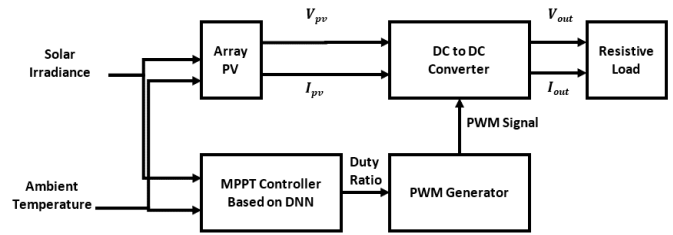


Figure 1. System configuration.

TABLE I  
SKYTECH SOLAR SIM-210 SPECIFICATION

| Property                              | Value     |
|---------------------------------------|-----------|
| Maximum power                         | 210 W     |
| Open-circuit voltage ( <i>Voc</i> )   | 30.58 V   |
| Short circuit current ( <i>Isc</i> )  | 8.8 A     |
| Voltage at MPP                        | 25.58 V   |
| Current at MPP                        | 8.26 A    |
| Temperature coefficient of <i>Voc</i> | -0.16%/°C |
| Temperature coefficient of <i>Isc</i> | 0.065%/°C |

irradiance data, the PV cell temperature value can be approximated using (1).

$$T_c = T_a + (T_{NOCT} - 20) \left( \frac{G}{800} \right) \tag{1}$$

where  $T_c$  is the cell surface temperature to be calculated;  $T_a$  is the ambient temperature to be converted;  $NOCT$  is the nominal operating cell temperature, which is equal to 45 °C; and  $G$  is the solar irradiance at the ambient temperature to be converted [13], [14]. Equation (1) can be represented as a subsystem in the form of a function block diagram. The PV array model used technical specification data from Skytech Solar SIM-210, as shown in Table I.

Next, the DC-to-DC power converter design was performed using three converter topologies: buck, boost, and buck-boost. Schottky diodes and MOSFETs were selected as switch regulators. The determination of converter inductance and capacitance parameter values for each topology is described in the following equations [8], [15], [16].

buck converter inductance:

$$L_{min\_buck} = \frac{D_{mpp}(1-D_{mpp})V_{mpp}}{f_s \Delta I_L} \tag{2}$$

boost converter inductance:

$$L_{min\_boost} = \frac{D_{mpp}V_{mpp}}{2f_s \Delta I_L} \tag{3}$$

buck-boost converter inductance:

$$L_{min\_buck-boost} = \frac{D_{mpp}V_{mpp}}{f_s \Delta I_L} \tag{4}$$

buck converter capacitance:

$$C_{min\_buck} = \frac{D_{mpp}(1-D_{mpp})V_{mpp}}{8f_s^2 L \Delta V_c} \tag{5}$$

boost converter capacitance:

$$C_{min\_boost} = \frac{D_{mpp}V_{out}}{2f_s R \Delta V_c} \tag{6}$$

buck-boost converter capacitance:

$$C_{min\_buck-boost} = \frac{D_{mpp}V_{out}}{f_s R \Delta V_c} \tag{7}$$

TABLE II  
 PV ARRAY AND CONVERTER PARAMETERS ON THE SIMULATION

| PV Arrays        |                  |                   |                     |                | Buck Converter |                   |                  | Boost Converter |                   |                  | Buck-Boost Converter |                   |                  |
|------------------|------------------|-------------------|---------------------|----------------|----------------|-------------------|------------------|-----------------|-------------------|------------------|----------------------|-------------------|------------------|
| $V_{mpp}$<br>(V) | $I_{mpp}$<br>(A) | $P_{mpp}$<br>(kW) | $R$<br>( $\Omega$ ) | $f_s$<br>(kHz) | $L$<br>(mH)    | $C$<br>( $\mu$ F) | $D_{mpp}$<br>(-) | $L$<br>(mH)     | $C$<br>( $\mu$ F) | $D_{mpp}$<br>(-) | $L$<br>(mH)          | $C$<br>( $\mu$ F) | $D_{mpp}$<br>(-) |
| 409.3            | 16.52            | 6.761             | 200                 | 30             | 0.5            | 20                | 0.898            | 2               | 30                | 0.648            | 4                    | 62                | 0.739            |

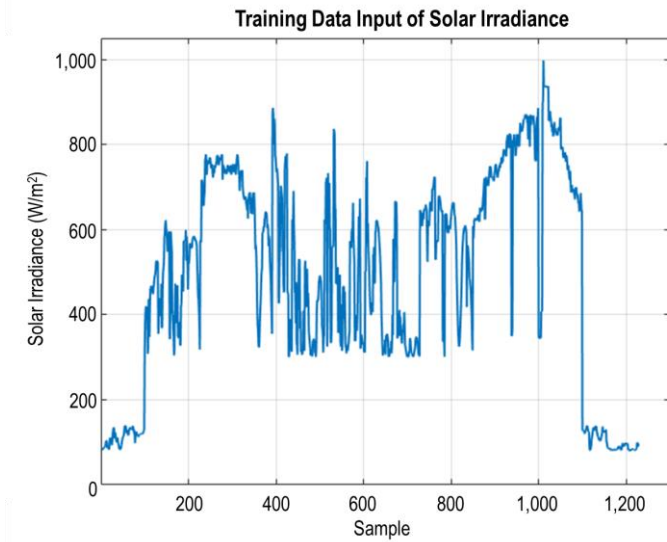


Figure 2. Input set of solar irradiance training data used for machine learning algorithm training data.

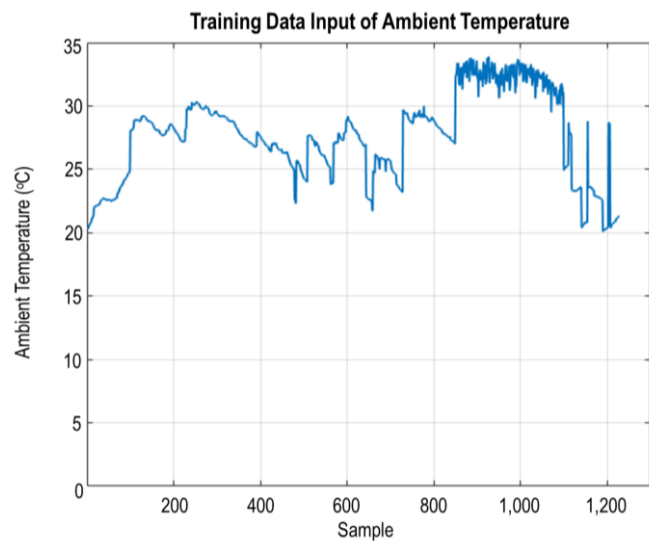


Figure 3. Input set of environmental temperature training data used for machine learning algorithm training data.

where  $L_{min}$  is the minimum inductance,  $C_{min}$  is the minimum capacitance,  $D_{mpp}$  is the duty ratio value at MPP,  $V_{out}$  is the converter output voltage,  $f_s$  is the switching frequency,  $R$  is the resistor resistance,  $\Delta V_c$  is the capacitor voltage ripple, and  $\Delta I_L$  is the inductor current ripple.

The capacitance and inductance parameters of each converter topology were obtained using (2) until (7), as shown in Table II. After designing the PV array model and DC-to-DC converter, the subsequent step was to build the MPPT control algorithm model. Two control algorithms, namely the InC and DNN algorithms, were compared. The InC algorithm with the hill climbing (HC) method was combined with a simple moving average (SMA) filter function block to generate the training data matrix used in modeling the machine learning

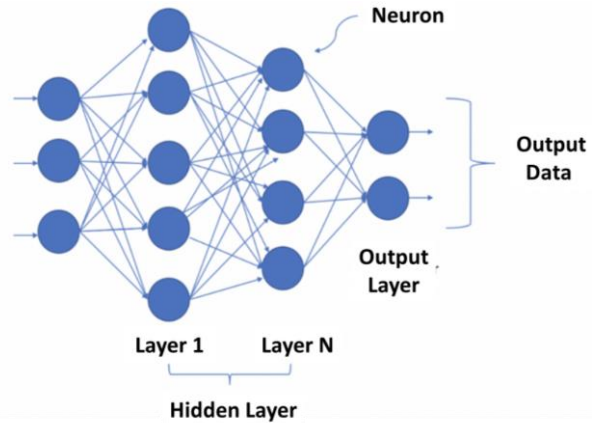


Figure 4. DNN architecture.

algorithm [17]. The training data generated by the InC algorithm are depicted in Figure 2 and Figure 3 as data plots.

These data were solar irradiance (W/m<sup>2</sup>) and ambient temperature (°C) on the PV modules that were connected to the InC controller. Next, InC formed the duty ratio and PWM as the switching signal required by the converter to reach the maximum power point.

Figure 4 shows the DNN architecture. It is evident that the input data served as input for neurons in the first layer, which provided output for other neurons in subsequent layers until producing a final output. The output was a prediction represented by probability (yes or no). Each layer could consist of one or more neurons. Each neuron computed a particular function, such as an activation function. The activation function would imitate the signal to be passed on as input to the neurons connected to the next layer. The relationship between neurons and successive layers is referred to as weight. This weight terminology defines an input's influence on subsequent neurons' output and, ultimately, on the final output as a whole. From the structural arrangement of DNNs, starting from neurons, layers, weights, input, and output, as well as activation functions, there is also a learning mechanism or optimizer that helps the neural network (NN) gradually update the weights so that they are suitable for making accurate predictions based on the final output produced.

Following the training data collection, the next stage was to design the machine learning algorithm model. The machine learning algorithm used was an NN-based algorithm with the Levenberg-Marquardt (LM) method [18]. In the algorithm training process, the training dataset was divided into three categories based on the rule of thumb: 70% for training, 15% for validation, and 15% for testing. The sum square error (SSE) value was calculated during the training process with the following equation.

$$E(x, w) = \frac{1}{2} \sum_{p=1}^P \sum_{m=1}^M e_{p,m}^2 \quad (8)$$

where  $x$  is the input vector;  $w$  is the weight vector;  $p$  is the pattern index, from 1 to  $P$ , in which  $P$  is the number of patterns;

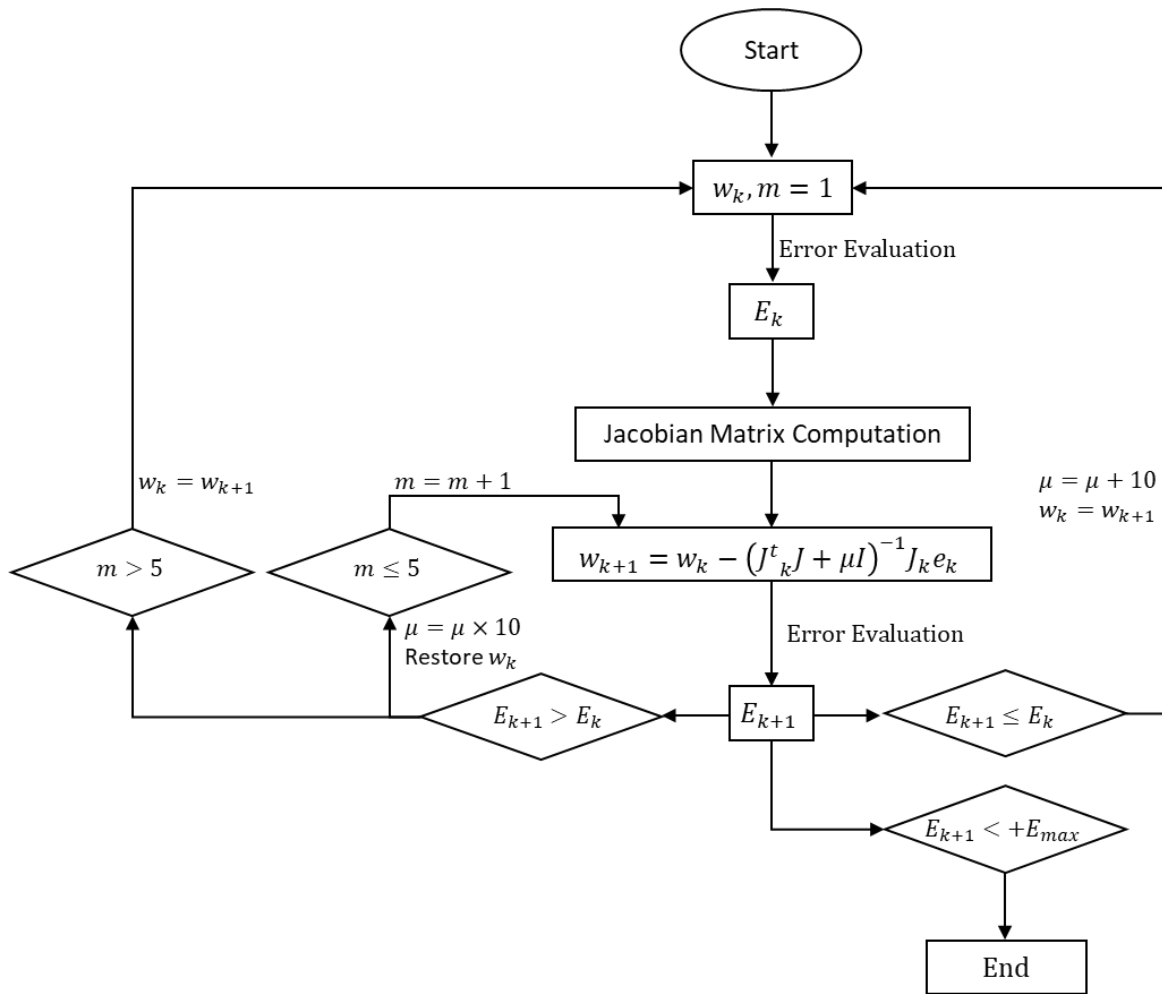


Figure 5. Flowchart of the training of NN algorithm with the LM method.

$m$  is the output index, from 1 to  $M$ , in which  $M$  is the number of outputs; and  $e_{p,m}$  is the training error at output  $m$  when using pattern  $p$  defined by (9).

$$e_{p,m} = d_{p,m} - o_{p,m} \tag{9}$$

where  $d$  is a vector of expected output and  $o$  is a vector of actual output.

SSE values were used in the steepest descent algorithm, which is a first-order algorithm that functions to find the minimum value in the error space. In modeling the NN algorithm with the LM method, the update rule in (10) was used.

$$w_{k+1} = w_k - (J_k^T J_k + \mu I)^{-1} J_k e_k \tag{10}$$

where  $w_k$  is the current weight,  $w_{k+1}$  is the net weight,  $e_k$  is the last overall error,  $J_k$  is the Jacobian matrix,  $I$  is the identity matrix, and  $\mu$  is called the combination coefficient which is always positive. The updating rule of the LM method used Jacobian matrix computation with the training block diagram shown in Figure 4.

Figure 5 depicts the training process utilizing the LM algorithm, beginning with providing random weight values and then using an update rule to obtain the desired SSE. The LM algorithm was combined with a bipolar sigmoid activation function (tansig), which accepted a matrix containing an input vector and then returned it to a matrix whose inputs had been previously suppressed to [-1 1] [19].

Mathematically, this function is not much different from the tanh transfer function. This tansig function can work faster than

the tanh function, but the numerical difference between the two functions is negligible. This tansig function is best used in the case of NN, where computational speed is more important than the exact form of the transfer function [20].

**C. PERFORMANCE TESTING SCENARIO**

In the validation and evaluation stage of the modeling and simulation performed, it is essential to observe the proximity between the power value generated by the PV array using DNN-based MPPT and the power value at MPP. The efficiency of an MPPT can be calculated by evaluating the ratio between the output power value to the MPP power [21], which can be mathematically written as follows.

$$\eta = \frac{P_{load}}{V_{mpp} \times I_{mpp}} \tag{11}$$

where  $\eta$  is the efficiency,  $P_{load}$  is the load power,  $V_{mpp}$  is the voltage at MPP, and  $I_{mpp}$  is the current at MPP. The higher the efficiency, the better the MPPT that is built. High efficiency indicates low losses that occur when the MPPT regulates voltage.

Other evaluation parameters that need to be considered besides efficiency are the accuracy of the algorithm in tracking the MPP, the computing speed of the MPPT algorithm, the speed at which the converter reaches a steady state, the presence or absence of oscillations in a steady-state condition, and the amount of undershoot or overshoot that occurs when there is a change in input [22]. The algorithm's accuracy can be calculated by comparing the amount of regulated PV voltage to the MPP voltage. Hence, the error can be calculated using (12).

$$error = \frac{|V_{pv} - V_{mpp}|}{V_{mpp}} \quad (12)$$

where  $V_{pv}$  is the PV voltage.

The computational speed of the MPPT algorithm can be determined by examining the computation time required until the MPPT obtains the reference duty ratio so that the voltage can be maintained at a particular value. Unlike the computational speed, the speed at which the converter reaches a steady state is not dependent on the MPPT algorithm but rather on the type of topology.

After constructing the model and determining the evaluation parameters, the next step was to test the PV array model and MPPT. The test was divided into two cases by applying the three built DC-to-DC power converter topologies: buck converter, boost converter, and buck-boost converter. The two cases are described below.

- Tests were conducted under standardized testing conditions (STC) at a solar irradiance of 1,000 W/m<sup>2</sup> and a cell temperature of 25°C.
- Testing of solar irradiance and ambient temperature was conducted in Bandung on Saturday, 11 June 2022 from 07:00 to 14:30.

### III. RESULT AND DISCUSSION

#### A. DUTY RATIO CALCULATION RESULTS

Before performing a DNN-based MPPT simulation, it is necessary to simulate using the HC method with the InC algorithm to acquire the duty ratio value as training data output. However, the InC algorithm-based MPPT provides a fluctuating duty ratio calculation. A simple filter in the form of SMA was utilized to eliminate the fluctuations and obtain a single duty ratio value that could be used as output in the training data. Figure 4 illustrates the simulation results in the form of duty ratio calculation for a PV array with InC algorithm-based MPPT and buck power converter under solar irradiance of 320 W/m<sup>2</sup> and ambient temperature of 28.1 °C that was simulated for 1 s.

Figure 6 demonstrates that the InC algorithm based MPPT produced a fluctuating duty ratio calculation with values ranging from 0.47 to 0.53. In order to train the DNN-based MPPT, one output value in the form of duty ratio was required under specific conditions of solar irradiance and cell temperature. So long as the duty ratio calculation is performed in the simulation, the SMA filter calculates the average duty ratio with a window of 12,000 until the filtered duty ratio calculation results are obtained, allowing a stable final value to be used as the output training data. After the filter process, the duty ratio value in the case of solar irradiance of 320 W/m<sup>2</sup> and cell temperature of 28.1 °C was found to be 0.491.

The accuracy of the calculated duty ratio value significantly affects the accuracy of the constructed DNN model. The greater the number and more precise the collected data, the better the trained DNN model. The three converter topologies were trained to obtain specific DNN models. Using the HC method with the InC algorithm, 1,228 training data were collected, and DNN-based MPPT was formed based on the training data. The training data were 1,228 × 3 matrices containing solar irradiance, ambient temperature, and duty ratio values.

The construction of the DNN's architecture required the inclusion of three layers: the input layer, hidden layer, and output layer. Prior to determining the number of hidden layers,

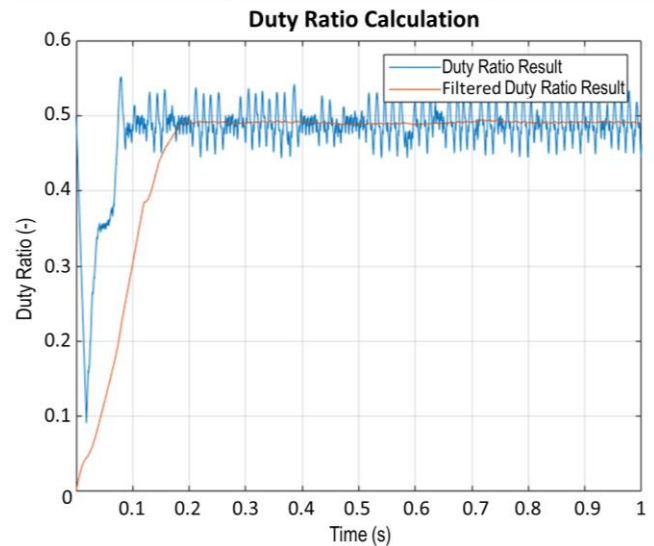


Figure 6. Comparison of duty ratio calculation before and after the filter process.

TABLE III  
 MSE VALUES AND TRAINING REGRESSION OF EACH CONVERTER TOPOLOGY

| Topology             | MSE ( $\times 10^{-5}$ ) | Regression |
|----------------------|--------------------------|------------|
| Buck converter       | 0.22                     | 0.9999     |
| Boost converter      | 2.27                     | 0.9985     |
| Buck-boost converter | 0.48                     | 0.9997     |

the DNN model underwent testing with a range of hidden layer spanning from 2 to 12.

Good training results have the smallest mean square error (MSE) value and a regression value close to 1. The smallest MSE values for training, validation, and testing were  $2.25 \times 10^{-5}$ ,  $2.27 \times 10^{-5}$ , and  $2.08 \times 10^{-5}$ , respectively. The three smallest MSE values were obtained from the test results of ten hidden layers. Meanwhile, the regression results, which is quite near to 1, for training were 0.9984. For validation, the results were 0.9885. These results were derived from test results with ten hidden layers. However, the best regression value for testing was 0.9987, which was acquired by testing three hidden layers. Thus, a DNN with ten hidden layers was selected. Each converter's topology was trained in order to get a specific DNN model for each of the three converters.

Table III presents the MSE calculation results, showing the validation performance of DNN and overall regression models for each converter. Buck converter has the best performance.

#### B. SIMULATION ON STC CONDITION

This simulation was performed by providing the PV array model with input values in the form of a constant value of solar irradiance of 1,000 W/m<sup>2</sup> and a constant cell temperature of 25 °C. Figure 7 and Figure 8 display the output power measurement results using MPPT with InC and DNN algorithms.

Figure 7 shows considerable oscillation in MPPT with the InC algorithm, which can be reduced by changing the algorithm to DNN, as depicted in Figure 8. In addition to eliminating oscillation, the time required for MPPT to attain a steady state can also be reduced. It can be seen that after reaching a steady state, the buck converter was able to keep the PV to provide the amount of power maintained at MPP, which was approximately 6,761 W. In the InC algorithm, the converter took longer than the DNN algorithm. It is due to the InC algorithm that must first evaluate the  $\frac{dP}{dV}$  value to determine the correct duty ratio value.

Measurement of Output Power in The PV Systems  
InC Algorithm

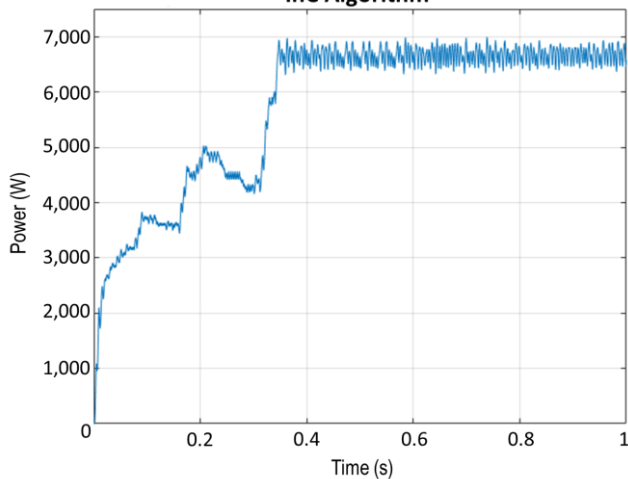


Figure 7. MPPT output power measurement graph of buck converter with InC algorithm.

Measurement of Output Power in The PV Systems  
DNN Algorithm

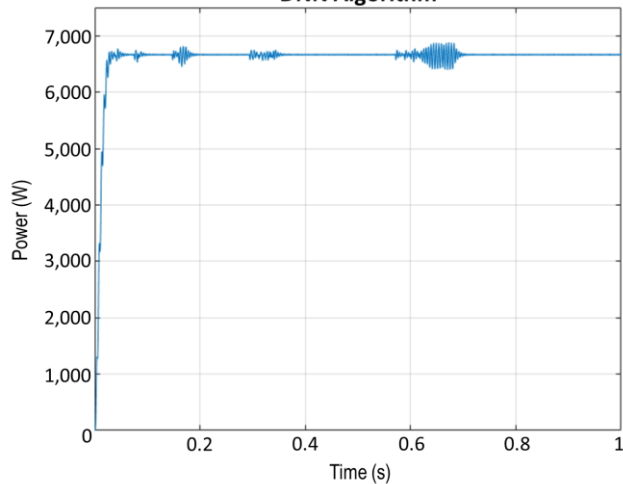


Figure 8. MPPT output power measurement graph of buck converter with DNN algorithm.

Since the DNN algorithm only provides one duty ratio value to the converter, the occurred oscillations can be significantly loss.

After attaining a steady state, the boost converter, like the buck converter, could maintain the PV so that it always supplied a large amount of power to the MPP, which was approximately 6,761 W. In quite extreme changes in solar irradiance, such as in the case of this STC test, allowing a change in solar irradiance from 0 W/m<sup>2</sup> to 1,000 W/m<sup>2</sup>, the boost converter provided quite large ripples before reaching a steady state until finally the existing ripples were significantly reduced.

More detailed calculation and evaluation results are presented in Table IV. This table gives a comparison of efficiency, voltage error, occurred oscillations, algorithm computation time, and settling time. It can be observed that by using the DNN algorithm, the efficiency of the buck converter at STC could be increased by 1%, and the time required to reach a steady state could be reduced by 88.17%. In addition, oscillations caused by the InC algorithm could also be eradicated by 1.5%, resulting in a reduction in losses. Meanwhile, in the boost converter, the efficiency could be

TABLE IV  
EVALUATION RESULTS IN STC CONDITIONS

|                       | Buck |      | Boost |     | Buck-Boost |      |
|-----------------------|------|------|-------|-----|------------|------|
|                       | InC  | DNN  | InC   | DNN | InC        | DNN  |
| Efficiency (%)        | 98.4 | 98.5 | 90.8  | 91  | 78.3       | 86.1 |
| Voltage error (%)     | 1.6  | 1.8  | 1.1   | 0.8 | 6.4        | 1.8  |
| Oscillation (%)       | 1.8  | 0.3  | 0.4   | 0.3 | 3.3        | 0.3  |
| Computation time (ms) | 347  | 3    | 269   | 3   | 327        | 3    |
| Settling time (ms)    | 361  | 42.7 | 295   | 181 | 384        | 316  |

increased by 0.2%, and the time required to reach a steady state could be reduced by 38.64%. The oscillations that occurred did not change significantly, but they were already relatively smaller. When compared to the buck converter, the boost converter had better accuracy, resulting in a high PV power supply and small oscillations. However, the efficiency of this topology is not the best, as it only reduced output power by 8.8%.

After testing, it is known that the buck-boost converter did not operate well enough when MPPT was simulated using the InC algorithm. Because the duty ratio range of this topology is smaller than the other two topologies, using the InC algorithm by taking a low step result in an error in finding the MPP duty ratio. Conversely, taking a high step result in irregular voltage oscillations, making it difficult to determine the duty ratio. The DNN algorithm only provided one duty ratio value upon evaluating the environmental conditions. This result can be seen from the large ripple during the missing steady state. Therefore, the DNN algorithm is better suited for the buck-boost converter.

It can be observed that the buck-boost converter provided a fairly stable output power, but it was not greater than the other two topologies. Due to the incompatibility of the buck-boost converter with the InC algorithm, the use of the DNN algorithm resulted in a 7.8% increase in high efficiency and a 4.6% reduction in the error of the regulated voltage value. The oscillations could be reduced by 3%, resulting in more stable power output, but the time taken by the buck-boost converter required the longest time compared to other topologies.

It can be concluded that the buck converter is the most efficient of the three converters, followed by the boost converter and then the buck-boost converter. Not only is the buck converter the most efficient, but it also reaches a steady state the fastest, whereas the buck-boost converter achieves the slowest speed. The accuracy and computational speed of the algorithm are not affected by the difference in converter topology. The three topologies also make no difference to the stability or oscillations present.

C. SIMULATION IN THE ACTUAL ENVIRONMENT CONDITION

The simulation was performed by inputting two signals, namely solar irradiance and ambient temperature, which were measured based on weather conditions on Saturday, 11 June 2022, from 07:00 to 14:30 Indonesia western standard time (waktu Indonesia barat, WIB) at Labtek VI, Institut Teknologi Bandung. The measured environmental conditions exhibited a solar irradiance range of 42 W/m<sup>2</sup> to 622 W/m<sup>2</sup> and an ambient temperature range of 20.4 °C to 29.2 °C.

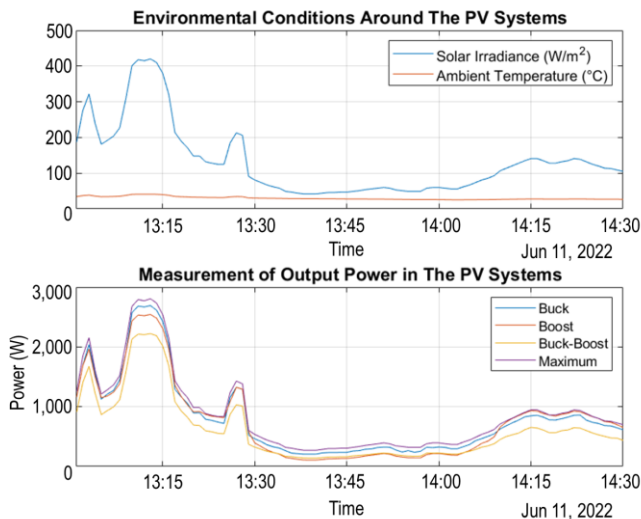


Figure 9. Measurement of power at 10:00–11:30 WIB.

Simulation results at 07:00 until 08:30 WIB showed that the power generated by the PV array with buck-boost MPPT had the lowest efficiency, while the buck MPPT consistently generated high efficiency. Unlike the others, the boost-topology MPPT exhibited both the highest and the lowest efficiencies. Under conditions of solar irradiance below 120 W/m<sup>2</sup>, the efficiency of the boost topology was observed to be at its lowest. This is owing to the limited operating range of the boost converter. The low irradiance prevents the converter from increasing the voltage to the maximum power point. On the contrary, when the received solar irradiance was greater than 120 W/m<sup>2</sup>, the boost converter could operate according to its capabilities and regulate the voltage at the maximum power point.

When measuring power by simulating environmental conditions between 8:30 to 10:00 WIB, the same result was discovered. Within the solar irradiance range of 100 W/m<sup>2</sup> to 230 W/m<sup>2</sup>, the buck-boost MPPT exhibited the lowest efficiency, whereas the boost and buck MPPT achieved the best efficiency.

Figure 9 depicts the test conducted between 10:00 and 11:30 WIB with a range of changes in sunlight irradiance between 180 W/m<sup>2</sup> to 600 W/m<sup>2</sup>. On the basis of observations on the converter output power against the incoming power in MPPT active mode, it can be determined that the buck topology was able to produce higher efficiency. At times, there was a sudden decrease in irradiance, such as at 10:45 WIB, when the buck converter briefly experienced a power decrease below that of the boost converter, followed by a gradual increase to a similar or slightly higher level. This condition stands in stark contrast to the buck-boost converter.

Furthermore, observations were conducted from 11:30 to 13:00 WIB. This observation range is intriguing, considering that the solar irradiance was at its peak during this time interval. The highest solar irradiance was reached at approximately 622 W/m<sup>2</sup> at 12:13 WIB, as shown in Figure 10. The output power measurement for each converter indicated that the buck converter was able to produce power closer to the MPP reference. In fact, it can be asserted that the output power in this condition is more consistent than the output power in the preceding time interval.

The solar irradiance gradually dropped significantly and did not peak again after 13:00 WIB. Figure 11 shows that this low

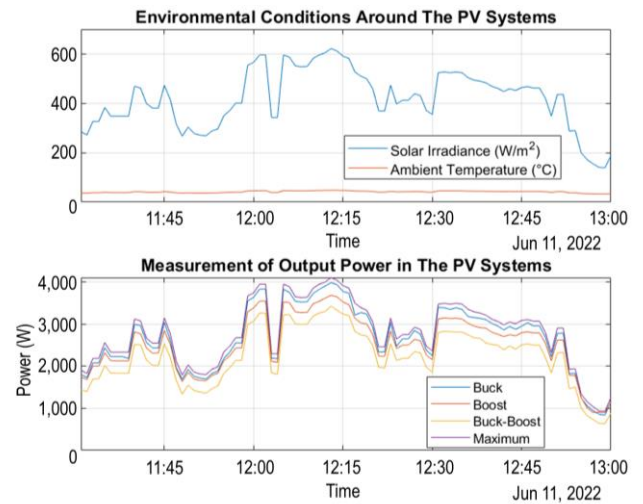


Figure 10. Power measurement from 11:30 to 13:00 WIB.

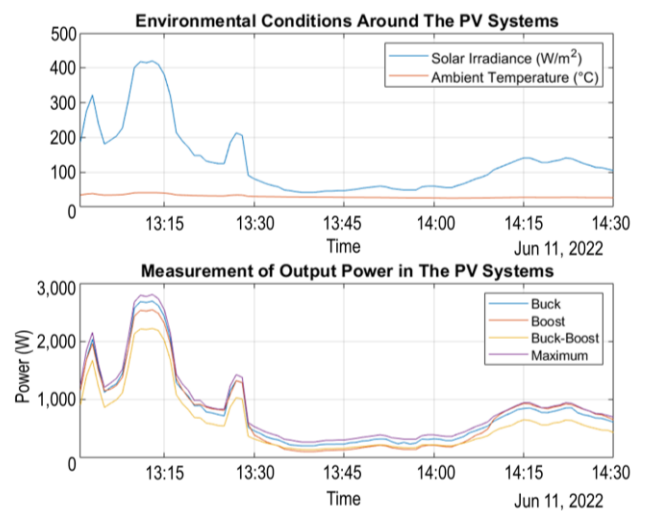


Figure 11. Power measurement from 13:00 to 14:30 WIB.

solar irradiance impacted the efficiency of the boost-topology MPPT, which was unable to operate at low irradiance.

Based on the descriptions from Figure 9 to Figure 11 presented above, performance testing of the three converters was conducted in the time window of 10:00 to 14:30 WIB, under irradiance and temperature conditions. The buck converter demonstrated higher performance than the boost and buck-boost. The buck converter voltage produced a lower value than the input, so intrinsically, the converter operated with lower voltage stress and lower switching losses. Boost and buck-boost converters tend to require voltage inversion, so the transfer of energy from the input to the larger output voltage results in increased losses and decreased efficiency.

#### D. MPPT EFFICIENCY

The efficiency value of the MPPT was quantitatively calculated for each topology operating under actual environmental conditions. The efficiency value was determined using (12), which was the comparison of the load power to the power attained at the maximum point or the amount of converter output power to its input power that should be achieved when activating the MPPT feature. The three converter topologies tested managed to reach the highest value in the time interval of 11:30 WIB to 13:00 WIB, which was 94.58% for the buck converter. On the other hand, the boost converter had a lesser efficiency of 90.79%. At the same time,

the buck-boost converter could only reach an efficiency of 79.34%.

It is worth noting that the difference in converter efficiency values is purely based on the performance alone. From a function standpoint, each converter possesses its own benefits. For instance, raising the voltage in the boost converter is a function the buck converter does not have. On the other hand, buck-boost converters exhibit lower efficiency. However, they functionally may be considered more favorable when dealing with cases necessitating voltage step-up and step-down tasks in a single converter.

#### IV. CONCLUSION

MPPT is a system that aids PV in tracking the maximum power point. The purpose of MPPT is realized through DC-to-DC power converters by applying the DNN algorithm. DC-to-DC power converter devices include buck, boost, and buck-boost converters. In conventional algorithm was used to obtain 1,228 training data in the form of duty ratio, which was obtained by providing input signals in the form of solar irradiance and ambient temperature. The training data were utilized to build DNN machine learning models for each modeled converter topology. The performance of the DNN model was validated using the MSE value criterion in buck, boost, and buck-boost converters, achieving values of  $2.20 \times 10^{-6}$ ,  $2.27 \times 10^{-5}$ , and  $4.80 \times 10^{-6}$ , respectively. The DNN algorithm could reduce oscillation effects, accelerate steady state time, and increase efficiency. The PV array using DNN-based MPPT was simulated under standard test conditions and actual conditions. The buck converter with the DNN algorithm achieved the best MPPT efficiency, amounting to 95.47%. The MPPT can consistently provide high efficiency under low and high solar irradiance. Meanwhile, MPPT with the boost converter and buck-boost converter yielded efficiencies of 90.97% and 79.34%.

#### CONFLICT OF INTEREST

The authors declare there is no conflict of interest in writing this paper.

#### AUTHOR CONTRIBUTION

Conceptualization, Edi Leksono and Irsyad Nashirul Haq; methodology, Robi Sobirin and Mochammad Iqbal Bayeqi; software, Putu Handre Kertha Utama and Muhammad Fatih Hasan; validation, Edi Leksono, Irsyad Nashirul Haq, and Justin Pradipta; formal analysis, Mochammad Iqbal Bayeqi and Muhammad Fatih Hasan; investigation, Reza Fauzi Iskandar and Putu Handre Kertha Utama; resources, Reza Fauzi Iskandar and Putu Handre Kertha Utama; data curation, Mochammad Iqbal Bayeqi and Muhammad Fatih Hasan; writing—original draft preparation, Robi Sobirin, Mochammad Iqbal Bayeqi, and Muhammad Fatih Hasan; writing—reviewing and editing, Robi Sobirin and Reza Fauzi Iskandar; visualization, Robi Sobirin and Muhammad Fatih Hasan; supervision, Edi Leksono and Irsyad Nashirul Haq; project administration, Mochammad Iqbal Bayeqi and Muhammad Fatih Hasan; funding acquisition, Irsyad Nashirul Haq and Justin Pradipta.

#### ACKNOWLEDGMENT

Authors would like to thank BPPT and LPDP as the funders who have provided support in this research.

#### REFERENCES

- [1] A. Haryanto, *Energi Terbarukan*, ed. 1. Yogyakarta, Indonesia: Innosain, 2017.
- [2] K. Amara *et al.*, "Improved Performance of a PV Solar Panel with Adaptive Neuro Fuzzy Inference System ANFIS Based MPPT," *2018 7th Int. Conf. Renew. Energy Res., Appl. (ICRERA)*, 2018, pp. 1098–1101, doi: 10.1109/ICRERA.2018.8566818.
- [3] V. Jatety *et al.*, "Experimental Analysis of Hill-Climbing MPPT Algorithms under Low Irradiance Levels," *Renew., Sustain. Energy Rev.*, Vol. 150, pp. 1–16, Oct. 2021, doi: 10.1016/j.rser.2021.111467.
- [4] K. Boudaraia, H. Mahmoudi, and A. Abbou, "MPPT Design Using Artificial Neural Network and Backstepping Sliding Mode Approach for Photovoltaic System under Various Weather Conditions," *Int. J. Intell. Eng., Syst.*, Vol. 12, No. 6, pp. 177–186, Dec. 2019, doi: 10.22266/ijies2019.1231.17.
- [5] M. Mao *et al.*, "Classification and Summarization of Solar Photovoltaic MPPT Techniques: A Review Based on Traditional and Intelligent Control Strategies," *Energy Rep.*, Vol. 6, No. 174, pp. 1312–1327, Nov. 2020, doi: 10.1016/j.egy.2020.05.013.
- [6] R.E. Idrissi, A. Abbou, and M. Mokhlis, "Backstepping Integral Sliding Mode Control Method for Maximum Power Point Tracking for Optimization of PV System Operation Based on High-Gain Observer," *Int. J. Intell. Eng., Syst.*, Vol. 13, No. 5, pp. 133–144, Oct. 2020, doi: 10.22266/ijies2020.1031.13.
- [7] H. Islam *et al.*, "Performance Evaluation of Maximum Power Point Tracking Approaches and Photovoltaic Systems," *Energies*, Vol. 11, No. 2, pp. 1–24, Feb. 2018, doi: 10.3390/en11020365.
- [8] R.F. Iskandar, E. Leksono, and E. Joeliando, "Q-Learning Hybrid Type-2 Fuzzy Logic Control Approach for Photovoltaic Maximum Power Point Tracking under Varying Solar Irradiation Exposure," *Int. J. Intell. Eng., Syst.*, Vol. 14, No. 5, pp. 199–208, Oct. 2021, doi: 10.22266/ijies2021.1031.19.
- [9] J. Chorfi, M. Zazi, and M. Mansori, "A New Intelligent MPPT Based on ANN Algorithm for Photovoltaic System," *2018 6th Int. Renew., Sustain. Energy Conf. (IRSEC)*, 2018, pp. 1–6, doi: 10.1109/IRSEC.2018.8702858.
- [10] A. Ab-Belkhair, J. Rahebi, and A.A.M. Nureddin, "A Study of Deep Neural Network Controller-Based Power Quality Improvement of Hybrid PV/Wind Systems by Using Smart Inverter," *Int. J. Photoenergy*, Vol. 2020, pp. 1–22, Dec. 2020, doi: 10.1155/2020/8891469.
- [11] A.A.M. Nureddin, J. Rahebi, and A. Ab-Belkhair, "Power Management Controller for Microgrid Integration of Hybrid PV/Fuel Cell System Based on Artificial Deep Neural Network," *Int. J. Photoenergy*, Vol. 2020, pp. 1–21, Dec. 2020, doi: 10.1155/2020/8896412.
- [12] M. Leelavathi and V.S. Kumar, "Deep Neural Network Algorithm for MPPT Control of Double Diode Equation Based PV Module," *Mater. Today Proc.*, Vol. 62, pp. 4764–4771, Mar. 2022, doi: 10.1016/j.matpr.2022.03.340.
- [13] G. Ciulla, V.L. Brano, and E. Moreci, "Forecasting the Cell Temperature of PV Modules with an Adaptive System," *Int. J. Photoenergy*, Vol. 2013, pp. 1–10, Sep. 2013, doi: 10.1155/2013/192854.
- [14] V. Sun, A. Asanakhm, T. Deethayat, and T. Kiatsiriroat, "A New Method for Evaluating Nominal Operating Cell Temperature (NOCT) of Unglazed Photovoltaic Thermal Module," *Energy Rep.*, Vol. 6, pp. 1029–1042, Nov. 2020, doi: 10.1016/j.egy.2020.04.026.
- [15] S. Thakran, J. Singh, R. Garg, and P. Mahajan, "Implementation of PO Algorithm for MPPT in SPV System," *2018 Int. Conf. Power Energy, Environ., Intell. Control (PEEIC)*, 2018, pp. 242–245, doi: 10.1109/PEEIC.2018.8665588.
- [16] S.K. Kollimalla and M.K. Mishra, "A Novel Adaptive P&O MPPT Algorithm Considering Sudden Changes in the Irradiance," *IEEE Trans. Energy Convers.*, Vol. 29, No. 3, pp. 602–610, Sep. 2014, doi: 10.1109/TEC.2014.2320930.
- [17] R. Rawat and S.S. Chandel, "Hill Climbing Techniques for tracking Maximum Power Point in Solar Photovoltaic Systems," *Int. J. Sustain. Develop., Green Econ.*, Vol. 2, No. 1, pp. 90–95, Jan. 2013.
- [18] A. Reynaldi, S. Lukas, and H. Margaretha, "Backpropagation and Levenberg-Marquardt Algorithm for Training Finite Element Neural Network," *2012 6th UKSim/AMSS Eur. Symp. Comput. Model., Simul.*, 2012, pp. 89–94, doi: 10.1109/EMS.2012.56.
- [19] A. Wanto *et al.*, "Levenberg-Marquardt Algorithm Combined with Bipolar Sigmoid Function to Measure Open Unemployment Rate in Indonesia," *Proc. 3rd Int. Conf. Comput. Environ. Agric. Soc. Sci. Health*

- Sci. Eng., Technol. (ICEST 2018)*, 2018, pp. 22–28, doi: 10.5220/0010037200220028.
- [20] M. Dorofki *et al.*, “Comparison of Artificial Neural Network Transfer Functions Abilities to Simulate Extreme Runoff Data,” *2012 Int. Conf. Environ. Energy, Biotechnol.*, 2012, pp. 39–44.
- [21] *Electrically Propelled Road Vehicles — Test Specification for Electric Propulsion Components — Part 7: Operating Load Testing of the DC/DC Converter*, ISO 21782-7:2021(E), 2021.
- [22] I. Owusu-Nyarko, M.A. Elgenedy, I. Abdelsalam, and K.H. Ahmed, “Modified Variable Step-Size Incremental Conductance MPPT Technique for Photovoltaic Systems,” *Electron.*, Vol. 10, No. 19, pp. 1–18, Sep. 2021, doi: 10.3390/electronics10192331.